

# Control Loop tuning by thermal simulation applied to the laser transformation hardening with scanning optics process

Silvia Martínez\*, Aitzol Lamikiz, Eneko Ukar, Iván Tabernero, Iñaki Arrizubieta

\* Corresponding author. E-mail address: [silvia.martinez@ehu.eus](mailto:silvia.martinez@ehu.eus); tel.: +34 94 601 7347; fax: +34 94 601 4215.

## HIGHLIGHTS

- Laser transformation hardening with scanning optics (LTHS) is a novel manufacturing process.
- A close loop temperature control for LTHS process has been developed.
- The control constants have been tuned by means of numerical thermal simulations.
- The developed method has been validated by comparing real and simulated results.
- Complex parts for the automotive industry have been hardened with the developed system.

**KEYWORDS:** Laser hardening; scanning optics; temperature control; thermal simulation; tuning.

## ABSTRACT

Laser transformation hardening with scanning optics (LTHS) is a novel manufacturing process on a very preliminary stage of introducing it in the surface treatment industry. The key to ensure the success in this process is the control of the process temperature. Thus, in this article, a close loop temperature control for LTHS process has been developed, tuned and tested in complex parts. On the one hand a PID temperature control has been implemented in a laser machine-tool. On the other hand, the same temperature control has been programmed in a numerical simulation software for LTHS process. In order to minimize experimental work, by means of using a novel method, the control constants have been tuned by means of thermal simulations. This method has been validated by comparing the results of the variation of different parameters in both cases, real and simulated. To complete the work, as the last test of the developed temperature control, different complex parts representing hardened parts for the automotive industry have been hardened with the developed system.

## Nomenclature

|           |   |
|-----------|---|
| $e_P$     | power error, W                                      |
| $e_T$     | temperature error, °C                               |
| $f_C$     | control frequency, s <sup>-1</sup>                  |
| $K_d$     | derivative constant                                 |
| $K_i$     | integrative constant                                |
| $K_p$     | proportional constant                               |
| LTH       | laser transformation hardening                      |
| LTHS      | laser transformation hardening with scanning optics |
| $P_a$     | actual power, W                                     |
| $P_{sp}$  | power set-point, W                                  |
| $t_C$     | control time, s                                     |
| $T_a$     | actual temperature, °C                              |
| $T_{max}$ | maximum temperature, °C                             |
| $T_{sp}$  | temperature set-point, °C                           |
| $V_F$     | feed rate, mm/min                                   |
| $V_S$     | scanning speed, mm/s                                |

## 1. Introduction

Laser transformation hardening (LTH) is a process based on a controlled heating and a later cooling of the surface, achieving a metallurgic transformation on the surface of the part. The heat source is a high power laser, since it is one of the most selective and controllable heat sources in the industry. The result of the process is the enhancement of the mechanical properties of the material, ensuring a higher wear resistance and an improved fatigue life creating a hardened and a compressive residual stresses layer in the surface [1]. Monitoring the process is essential since the temperature on the surface must be always below the melting point but higher than the transformation temperature. The temperature control also becomes a difficult task due to the interdependence of the mechanical properties, the microstructure and the temperature field in the process. This relationship is called Metallo-Thermo-Mechanical coupling and a deeper study of the effects can be find in [2]. Thus, Yislab et al. [3] although study the interdependence between the temperature field and thermal stress field during a laser process.

The introduction of a control algorithm on the temperature enables the automation of the LTH process as the material has the proper metallurgical distribution and adequate mechanical properties, regardless the geometry or the material of the part. One of the main objectives for controlling the temperature of the process is the necessity of adjusting the parameters of the process to unexpected conditions, such as variation in roughness or geometry. If the laser power is set constant, the temperature could vary significantly near part corners or edges. Sometimes to avoid this effect a thermal camera is needed. Laser hardening process is used in the industry for surface hardening of small parts, bearing and ball screw races, die & molds, etc. All these applications need a passive or active temperature control in order to maintain the same treated area properties regardless the geometry of the part. Seifter et al. [4] calibrate temperature measurement devices for laser heat treatments.

Laser hardening process is gaining industrial interests in the last years, since it is possible to process complex 3D shapes with a minimum heat affected zone and thermal distortions in comparison with more traditional hardening techniques. Propawe in [5] shows equipment requirements and different applications of laser hardening process.

Furthermore, in recent years a series of systems based on moving optics for guiding high power lasers are being developed and industrialized. These systems are also called scanners and they are usually coupled to the wrist of a serial robot [6] or in the spindle of a machine tool [7]. The main characteristic of the scanners is the ability to move and guide the laser beam with very high accuracy and speeds (above 10,000 mm/s). The agility of the movements is obtained by the rotation of two mirrors with very low mass and inertia. Thus, these rotations are converted into very fast linear movements in the part, corresponding with X and Y axes. In Fig. 1a) a 2D scanner scheme is shown. The main advantage of scanners is the high processing speed and the working distance, which use to be far from the area to be processed, being able to process difficult-to-access zones maintaining the quality of the laser beam. Díaz-Tena et al. [8] use an industrial high power laser beam with scanning optics to provide a rapid and free form engraving on a resin mask without affecting the specimen surface.

At the present, there are several emerging industrial processes based on the use of scanners in different manufacturing areas, particularly in the automotive industry, such as remote laser welding or large areas marking with moving scanner optics. Gradually these systems are being introduced in other industrial sectors such as the die and mold manufacturing industry where laser remote processes are being applied for

texturing [9], polishing [10] or drilling [11]. In contrast, remote treatment processes development is still on a very preliminary stage, with some research performed to evaluate the process capabilities [12, 13].

As it can be observed in Fig. 1b), laser transformation hardening with scanning optics process (LTHS), presents a combination of two speeds: the scanning speed and the machine feed rate. The characteristic parameter of this process is the scanning speed ( $V_S$ ), usually measured in mm/s representing the guiding speed of the laser beam. This speed need to be very fast, since the treated area is defined by this laser sweep, therefore  $V_S$  is controlled by the mirrors of the scanner and it can reach up to 10,000 mm/s. Furthermore there is a feed rate ( $V_F$ ), measured in mm/min, which is the federate motion of the robot or machine tool and represent the speed of the laser sweep line translation.

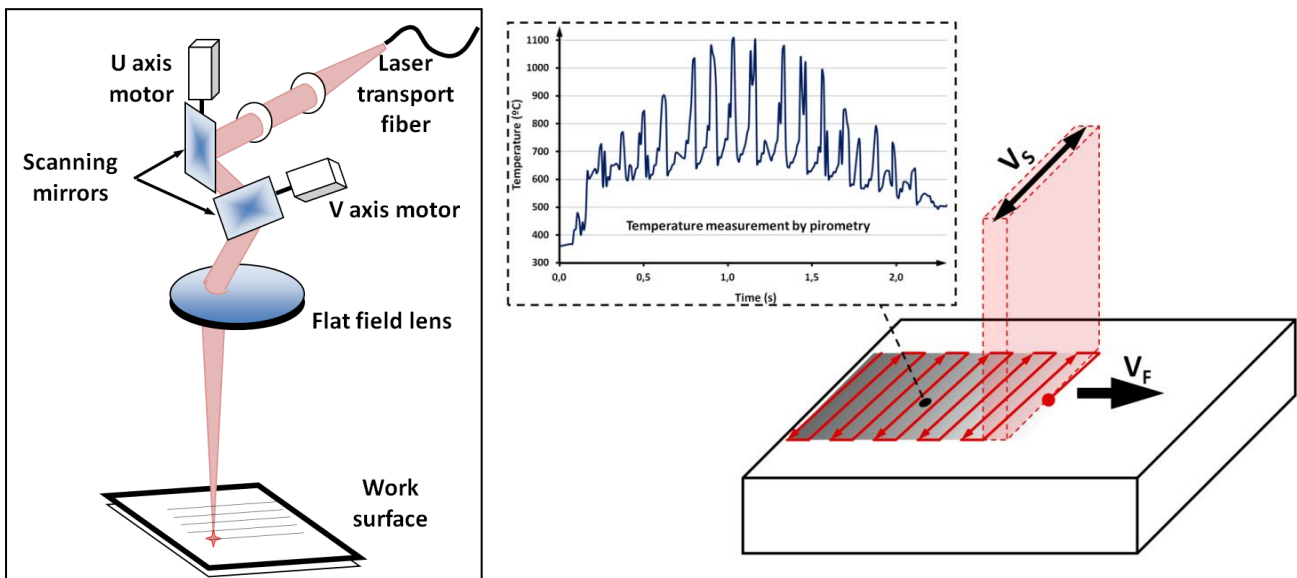


**Fig. 1 a) A 2D scanner components; b) Thermal field generated in a part point.**

In addition, the interest of laser hardening process lies in the possibility of direct integration of a very flexible laser heat source on the production line without a quenching medium, as well as the possibility to produce different microstructures in the part getting a soft core with a hardened surface layer with compressive residual stresses. During laser hardening process fixed optics are needed to find the optimal intensity distributions of the transformed laser beam that could produce the target transient temperature fields in the part. In [14] a laser Gaussian beam was transformed into concentric multi-circular patterns by means of a high cost diffractive fixed optic to produce a shaped thermal load. However, LTHS process presents the same advantages than laser hardening but the optics can be programmed to different track widths. In addition, solid state lasers such as fiber or disk lasers can be used for hardening while conventional laser hardening is only performed with direct diode lasers.

One of the most relevant aspects on LTHS is the in-process temperature control requirement. The process temperature must be verified during the whole process in order to avoid surface melting. The temperature control becomes harder if the laser beam moves rapidly, so the tuning of the temperature control loop is one of the most challenging aspects on the LTHS process. In all the implemented controls a non-contact temperature measurement technique is been used, such as pyrometers or thermographic cameras. Purtonen et al. [15] review the different sensors used for monitoring laser processes.

The main advantage of the pyrometers is their rapid response as well as the capability of not interfering in the process. There are several types of pyrometers, being ratio pyrometer (also known as 2-color-pyrometer) one of the most widely used for laser surface treatment processes. These pyrometers measure IR radiation at two different wavelengths and by doing so the temperature becomes independent of the emissivity of the object. The main drawback of the pyrometers for laser surface treatment processes is that measure of the temperature is limited to a single point. For a continuous temperature measurement in the treated area, thermographic cameras are needed but these systems are still very expensive and an emissivity calibration is necessary before its application [16].

Once one way of measuring the temperature is decided, the control system has to be implemented somewhere. The most robust way is hardware based control system, which offers a more rapid response but less flexibility. Most of the practical approaches implement a PID (Proportional Integral Derivative) temperature control and tuning its parameters by means of experimentation. Therefore, the simulation of the laser hardening process becomes a major asset when adjusting the parameters of the control since experimentation is not always possible. Tuning of the control system can be expressed as an optimal control problem, which aims at minimizing the difference between the actual microstructure distribution and the desired one by taking into account the constraints of the process [17]. Further question arises on which temperature should be measured. Some researches propose a sophisticated control [18], which aims at keeping a constant temperature of the material at the bottom of the hardened layer.

Furthermore, the numerical thermal simulation of manufacturing processes with high power lasers is a realistic method to simulate, predict and know important parameters as the temperature during processes. And it can be solved by means of a lot of different methods. For example, Sincovics et al. [19] use thermal cell method to develop a model of the laser ablation of polymers. Finally, although some analytical method could be utilized, Amine et al. [20] investigate the effect of process parameters on multilayer direct laser deposition process and Yuan et al. [21] solve the temperature field of a film photovoltaic cell under laser irradiation by means of 3D Finite Element Method.

In this article, a close loop temperature control for LTHS process has been developed. It has been tuned and tested in complex parts. On the one hand a PID temperature control has been implemented in a laser machine-tool. On the other hand, the same temperature control has been programmed in a numerical model for LTHS process. The result is a virtual PID control integrated into the simulation model that can be used for tuning the PID algorithm by means of thermal simulations. The tuning strategy is based on the proposed by Ziegler-Nichols [22]. A similar approach has been presented by Devesse et al. [23] for laser cladding process but without experimental validation.

Therefore, the main objective is to minimize experimental work and adjust the PID control for each set of material and laser parameters. This method has been experimentally validated by comparing the results of the variation of different parameters in both cases, real and simulated. Finally, a complex test part representing a typical die for automotive industry has been hardened with the developed system.

## **2. Temperature control implementation**

Since the laser beam sweeps the treated surface, the temperature ripple during LTHS process is inevitable and intrinsic to the process. To understand better the thermal process in the part, a deeper analysis of the temperature field during LTHS process shows two different process regimens depending on the scanning speed, considering the same feed rate ( $V_F$ ). In order to analyze the process regimes more

deeply, the Temperature - Time - Position evolution in different zones of the scanned lines has been obtained by means of the simulation of the temperature field. As it is shown in Fig. 2, at low scanning speeds, temperature peaks at the terminations are higher than the central point and the temperature ripples are more significant. If the scanning speed is increased, the simulation shows that the maximum peak of temperature is at the center of the scanning line. Moreover, the temperature signal is smoother while the ripples are attenuated.

These regimes present also two different shapes of the hardened layer. The first one, the rippled state shown in Fig. 2a), can be found at low scanning speeds, and presents an almost constant thickness but with the maximum hardened thickness near the side limits. By contrast, the continuous regime shown in Fig. 2b), is achieved at high scanning speeds and presents a hardened layer shape similar to the conventional laser hardening process, with a semi-elliptical shape with the maximum hardened thickness in the center of the line.

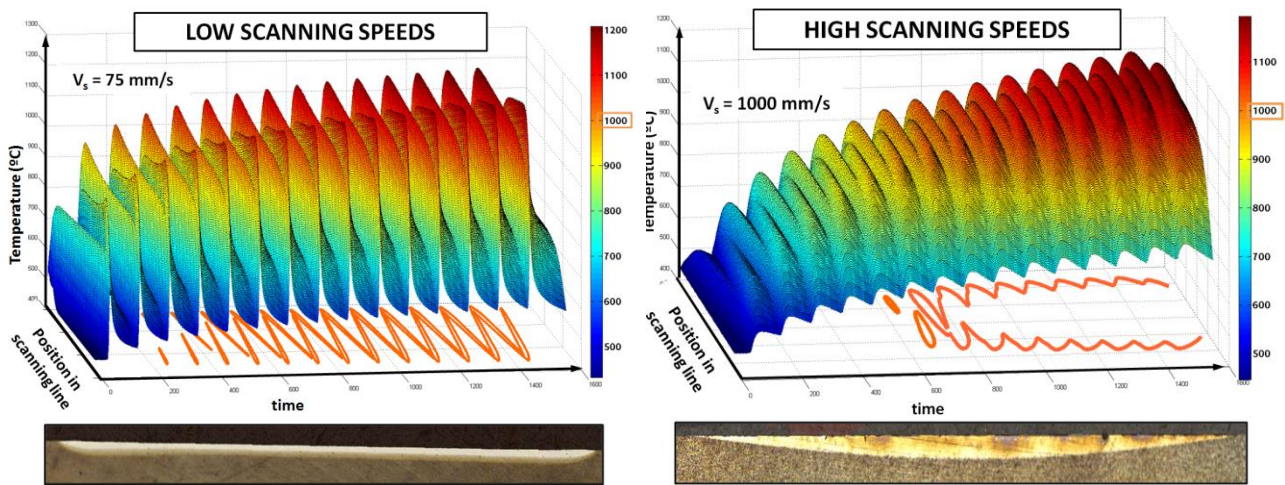


**Fig. 2 a)** Temperature and hardened layer in the rippled regime; **b)** Temperature and hardened layer in the continuous regime.

The temperature ripples in the surface cause a high variable temperature on the part surface, which results on a more difficult temperature measurement and control. It can be minimized by increasing scanning speed, but never avoided. Thus, in Fig. 3 b) different temperature measurements for a single test are shown. The dashed line, corresponding to the temperature of the laser beam, and it is referred to the maximum temperature during the process. In order to keep it constant, the 2-color-pyrometer should be guided to follow the laser beam optical path but, as previously mentioned, it is not possible without positioning errors. The continuous line represents the temperature measured by the pyrometer that moves joined to the machine-tool head at a constant feed rate ( $V_F$ ) as is it shown in Fig. 3a). The ripple of the temperature measured by the pyrometer is higher than the laser beam temperature. Therefore, the pyrometer has been programmed to store only the peak of all the temperature values measured during the control cycle.

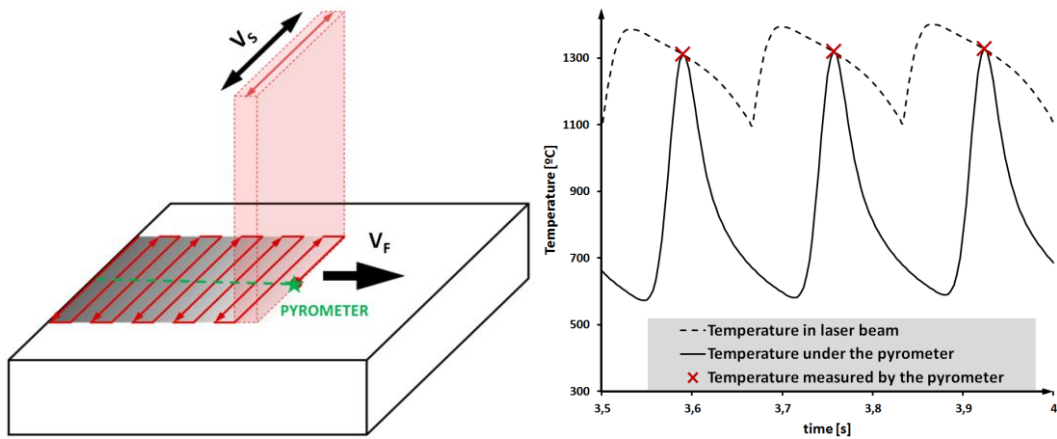


**Fig. 3 a)** Pyrometer position during LTHS process; **b)** Different thermal field generated in the part.

Moreover, the analysis of the areas where the maximum average temperature will be achieved is a key factor for the positioning of the pyrometer in order to control the process. Therefore, for high scanning speeds (higher than 750 mm/s), it is shown in Fig. 2 that the optimum positioning of the pyrometer is the center of the track, whereas for low scanning speeds (lower than 200 mm/s) it is recommended to measure the temperature near one of the terminations of the track.

The LTHS manufacturing system consists of the joining of the process and the control. Moreover, in an active or close loop control each control time, ( $t_c$ ) a parameter transfer between process and control is performed. Thus, in the developed close loop control, each  $t_c$ , the control gets the actual temperature value and, after the processing, a power parameter value is sent to the laser. The real temperature control parameters are taken from the simulated system as it is shown in the diagram of the Fig. 4. The temperature control for the experimental tests used the measured temperature by the pyrometer as input and evaluates a new laser power value. On the other hand, the control algorithm needs to be tuned in order to obtain smooth laser power signals. Thus, simulated temperature is used for the PID tuning using virtual control algorithm.

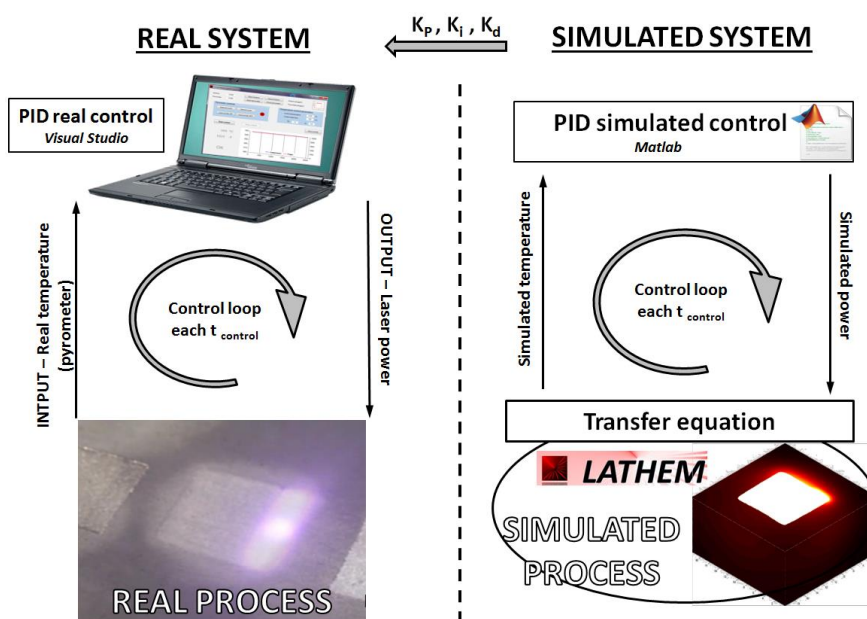


**Fig. 4** Diagram showing the relationship between real system and simulated system.



By means of the simulated system the required tests for the setting of the real control parameters are avoided or minimized. The system simulation can be carried out through different techniques as is shown in [24], but all of them are based on the process transfer equation. In this case, a numerical thermal model discretized in time and space is used as a simulation of the real process in order to obtain the LTHS process transfer equation. In other words, it is a realistic way to give a temperature value on the part surface as function of the laser power. A numerical simulation program and an inverse problem knowing the real temperature on a discrete point of the part is a reliable method of simulating the temperature field in the whole part as is shown in [25].

Once the main basics of the system have been described, in the following sections the PID controller, the real system implementation, the thermal simulated system and the control constants tuning will be described.

## 2.1 PID temperature controller

Proportional-integral-derivative (PID) control is by far the most widely used form of feedback control [26]. In a PID control, the error signal is a sum of three terms: proportional action (P) which refers to actual values, integral action (I) which eliminates past errors in the steady state and derivative action (D) which anticipates the future error. In Fig. 5 the blocks diagram of the PID controller implemented in the real system is shown. The time between each control step is the control period,  $t_c$ .

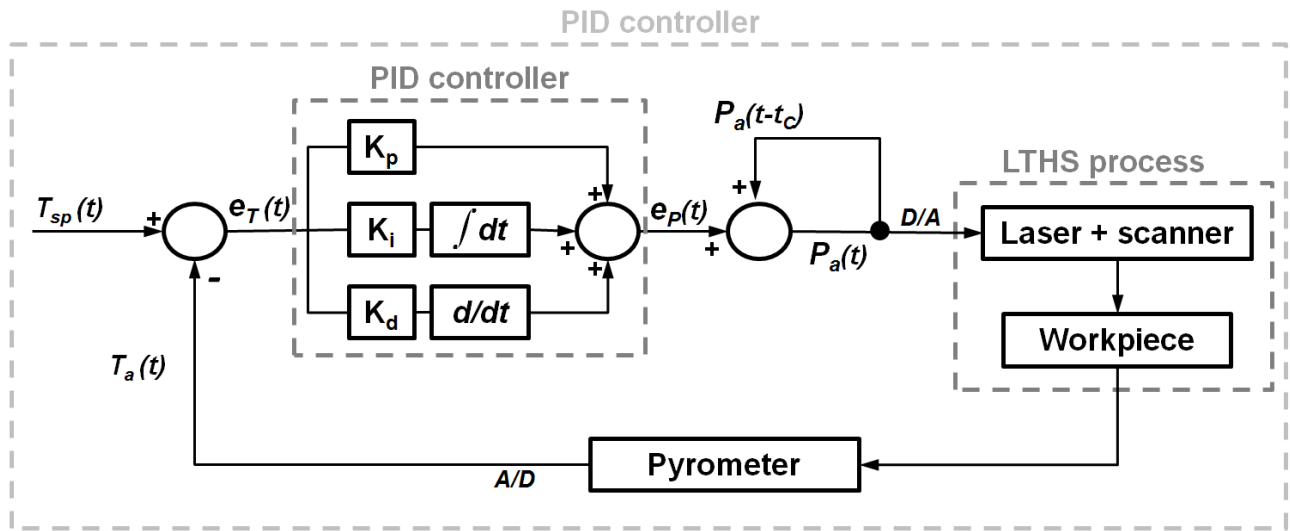


Fig. 5 Real system block diagram.

The time dependant PID control equation is a sum of the three terms. For LTHS process control development the control result is given as a power error ( $e_p$ ):

$$e_p(t) = K_p e_T(t) + K_d \frac{de_T(t)}{dt} + K_i \int_0^t e_T(t) dt \quad \text{Eq. 1}$$

where  $e_p$  is the power error,  $e_T$  is the temperature error and  $K_p$ ,  $K_i$  and  $K_d$  are the PID control constants. The temperature error signal ( $e_T$ ) is the difference between the actual value and the reference value that is called the set point.

$$e_T(t) = T_{sp}(t) - T_a(t) \quad \text{Eq. 2}$$

In order to implement this algorithm on a digital system and to control dynamically the process, the time dependent Eq. 1 has to be modified as a discrete equation. For this purpose, the control frequency,  $f_c = 1/t_c$ , has been introduced. Thus, the derivative and the integrative approximations get:

$$\frac{de_T(t)}{dt} \approx (e_T^n - e_T^{n-1}) * f_c; \quad \int_0^n e_T(t) \approx \sum_{j=0}^{n-1} e_T^j * \frac{1}{f_c} \quad \text{Eq. 3}$$

Adding terms to Eq.1:

$$e_p^n \approx K_p e_T^n + K_d f_c (e_T^n - e_T^{n-1}) + \frac{K_i}{f_c} \sum_{j=0}^{n-1} e_T^j \quad \text{Eq. 4}$$

To obtain a more compact equation the previous step equation is subtracted:

$$e_p^n - e_p^{n-1} \approx K_p (e_T^n - e_T^{n-1}) + K_d f_c (e_T^n - 2e_T^{n-1} + e_T^{n-2}) + \frac{K_i}{f_c} e_T^{n-1} \quad \text{Eq. 5}$$

$$e_p^n = e_p^{n-1} + q_0 e_T^n + q_1 e_T^{n-1} + q_2 e_T^{n-2} \quad \text{Eq. 6}$$

where  $q_0 = K_p + K_d f_c$ ,  $q_1 = -K_p + K_i f_c^{-1} - 2K_d f_c$  and  $q_2 = K_d f_c$ ;  $f_c$  is the control frequency and the  $t_c$  inverse.

In order to control the LTHS process, a conventional PID control loop has been purposed. The PID algorithm is based on 3 parameters that must be adjusted for each material and process parameters combination. Typically, the constants tuning is made by trial-and-error techniques, which result on long testing periods. Therefore, this work purposes a numerical model of the LTHS to tune the PID constants and finally adjust the PID algorithm for the process. The numerical model of the LTHS process estimate the resulting temperature for different laser powers, and the estimated temperature is used as input for the PID. Thus, different PID algorithms are tested virtually instead of performing real tests for each material and parameter combination. In summary, the tuning procedure by means of numerical simulations that will be explained in section 2.4 is the main goal of this research.

## 2.2 Real system configuration

All the experimental tests have been developed with a 1 kW fiber laser guided with a 2D scanning head. The scanning head is attached to a conventional machine-tool which moves the scanner at a  $V_F$  speed. In Fig. 6, a diagram of the close loop temperature control developed for LTHS is shown. The temperature during the process is measured without contact with a 2-color-pyrometer that gives the actual value of the temperature without having to know part emissivity [27]. Then, the temperature of the part surface is stored in a computer and compared with the reference temperature. The error in temperature is used as input value for a digital PID control that adjusts and obtains an error on laser power, Fig. 6. That power variation is added to the previous cycle value and is sent to the laser generator. Thus, a laser beam with the required power is guided by a fiber to the scanner. The scanner moves the laser beam to the corresponding point in the part surface heating it and the control loop is closed.



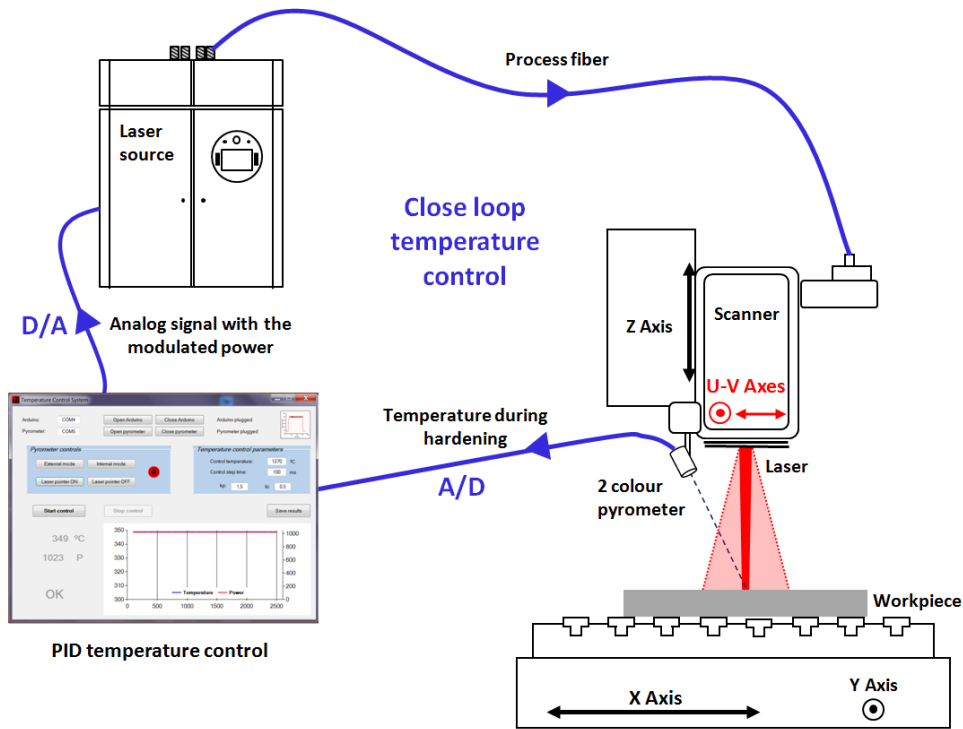


Fig. 6 Real system components diagram.

Different LTHS tests with the implemented system and different process parameters were carried out. This tests results are shown in Fig. 7a). In Fig. 7b) the power variation given by the control to keep a temperature set-point of 1,250 °C during a test is shown in more detail. It can be observed that a higher power at the beginning was needed. Once the temperature is achieved, an almost constant power in the intermediate zone of the track and, finally, a decrease of the laser power in the exit of the part can be observed. These measurements were performed by positioning the pyrometer always in the center of the track that was being scanned.

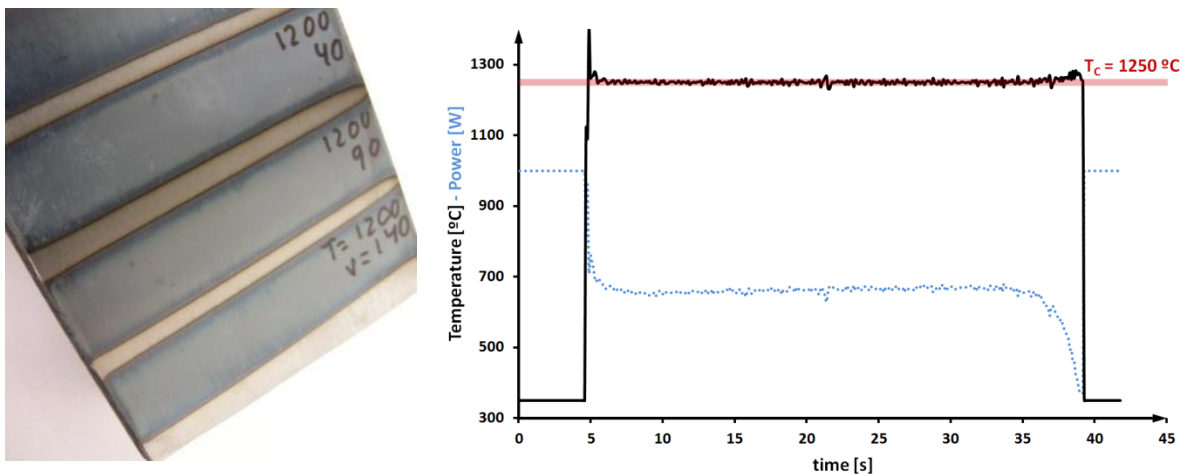


Fig. 7 a) Temperature control result in tests with different feed rates; b) Power variation with the implemented temperature control during a LTHS test;  $T_{SP} = 1,250 \text{ } ^\circ\text{C}$ .

### 2.3 Thermal simulated system

Thermal simulated system is composed by the simulated process and the simulated control algorithm. Thus, in the simulated control system the Eq. 6 has been programmed in the same manner as in the real system. The entire simulated system was programmed in Matlab® software.

The LTHS process simulation was performed based on LATHEM (LAsEr\_THERmal\_Model) program [28]. LATHEM is a thermal model based on the differential equation for heat transfer by conduction. The differential equation is solved by Central-Finite-Difference method which in the case of the thermal field simulations is put into an explicit expression, solved with a low computational cost.

In addition this program includes the energy consumption during material heating in the solid state phase transformations by means of Johnson-Mehl-Avrami equation.

For programming the simulated system the block diagram shown in Fig. 8 a) was followed. LATHEM is fed by the accumulated power coming from the simulated control. Maximum laser power is set for the first simulation step. After a simulation time equal to the control time ( $t_c$ ) the maximum simulated temperature value under the pyrometer position ( $T_a$ ) is stored. The difference between this temperature and the temperature set-point ( $T_{sp}$ ) is used for taking the temperature error ( $e_p$ ) and it is used as the input of the next simulation cycle to the control. These steps are carried out for the LTHS test through the entire laser beam trajectory. The total number of simulated steps was about 10,000 steps and the global simulation time in these tests was about 21 minutes per test.

In Fig. 8 b) the resulting simulated thermal fields on two parts with different thickness are shown. In both cases the temperature control was simulated and the hardening temperature in the part surface is the same but the hardened shape is different due to the differences on the heat dissipation characteristics as well the amount of heat accumulated.

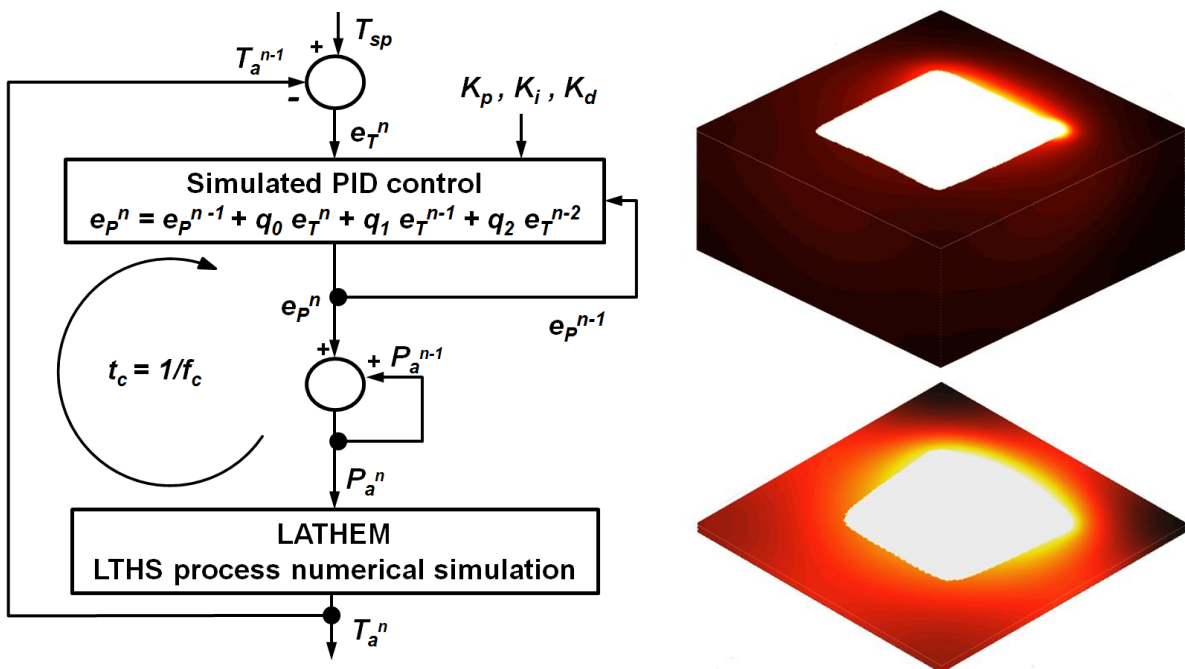


Fig. 8 a) Simulated system block diagram; b) Thermal field simulated results on different thickness parts.

## 2.4 LTHS temperature control tuning

In this section the LTHS temperature control tuning will be explained. For this purpose, the control constants adjustment has been carried out by means of the simulated system. After the tuning, with the aim of validate the full method, different tests with the real system on flat part geometry were performed and compared with the simulated ones.

A brief explanation of the steps followed during the constants tuning are detailed next.

- First, the integrative and derivative constants were programmed to zero while the proportional constant was increased from a very low value until it reached a limit value at which the output signal, laser power, ranged between a minimum and a maximum value. In Fig. 9 the simulated graphs in the first step with the proportional constant in its limit value ( $K_p = 3$ ,  $K_d = 0$  and  $K_i = 0$ ) is shown with the results of these conditions in a real part. Thus, the proportional constant was set to approximately the 60 % of the limit value.

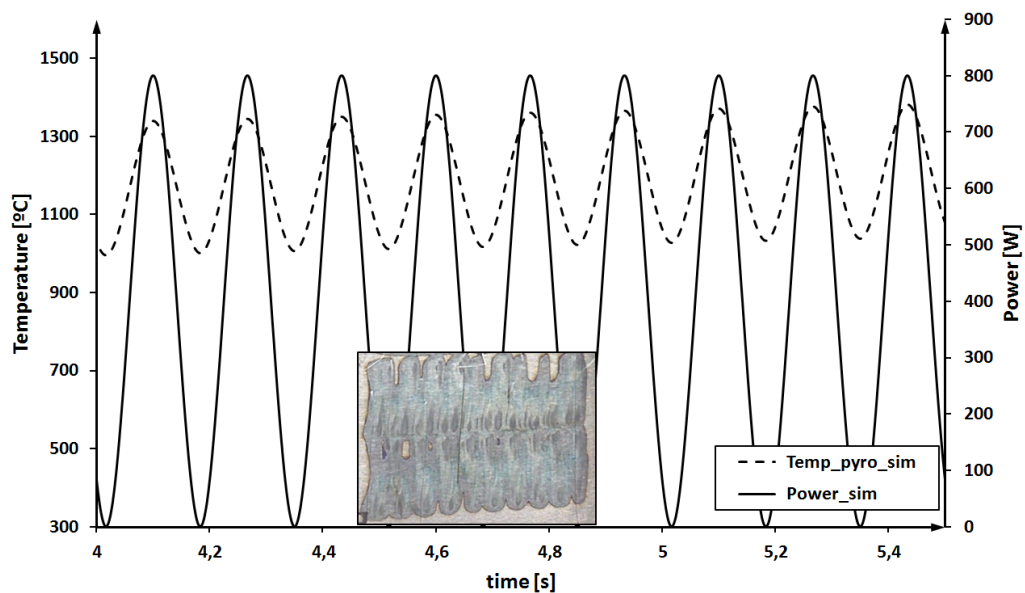


**Fig. 9** Simulated temperature and power graphs during the tuning. First step with  $K_p = 3$  (limit value),  $K_d = 0$ ,  $K_i = 0$  and  $P_{sp} = 800$  W.

- Next, the integrative constant value was increased until the output temperature in the steady state reaches the temperature set-point.
- Finally, the derivative constant value would have been increased to be quick enough to reach the temperature set-point after a sudden temperature variation.

## 2.5 Validation tests

Once the control tuning of the PID is carried out, an experimental validation has been performed. The validation has been carried out with a conventional AISI 1045 structural steel as part material. The material, laser power, process speeds and control parameters used are shown in Table 1.

**Table 1** Parameters used during the validation tests.

|                                 |              |
|---------------------------------|--------------|
| Material                        | AISI 1045    |
| Power set-point, $P_{sp}$       | 500 W- 800 W |
| Scanning speed, $V_S$           | 1,000 mm/s   |
| Feed rate, $V_F$                | 60 mm/min    |
| Temperature set-point, $T_{sp}$ | 1,200 °C     |
| Proportional constant, $K_p$    | 1.6          |
| Derivative constant, $K_d$      | 0.05         |
| Integrative constant, $K_i$     | 0            |

The first LTHS validation test was carried out without temperature control (Fig. 10). During real test and simulated test the power was kept constant and the temperature increased continuously. The part surface changed from no hardening at the beginning of the test up to melting the material at the last steps of the test. In the real temperature graph a section with a constant temperature is observed. This is due to the pyrometer measurement limit is located at 1,350 °C, so it is over-ranged.

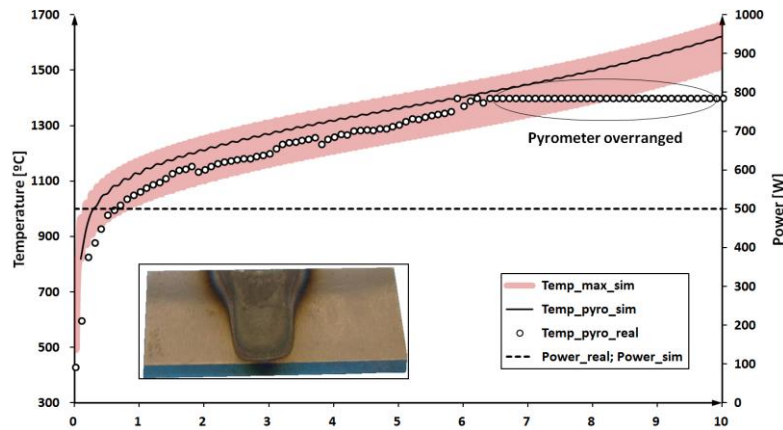


**Fig. 10** Real/simulated temperature and power graphs during a test without temperature control and  $P_{sp} = 500$  W.

The second LTHS validation test was carried out with the tuned control parameters shown in Table 1. The resultant temperature and power graphs are shown in Fig. 11. Simulated and real graphs present similar values and trends. The power through the test decreases because the part is gradually heated and, therefore, less power is needed to maintain a constant temperature on the surface. In addition, the actual temperature reaches quickly the temperature set-point and the peak in the test beginning is not too high to melt the part surface.

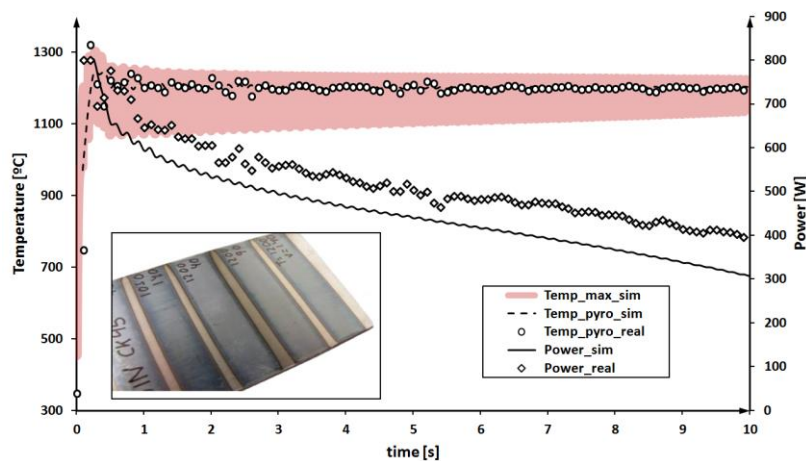


**Fig. 11** Real/simulated temperature and power graphs during a test with  $K_p = 1.6$ ,  $K_d = 0.05$ ,  $K_i = 0$  and  $P_{sp} = 800$  W.

To conclude, tests modifying different LTHS process parameters were performed. For example, programming the power set-point with a very low value (500 W in order to 800 W), which would lead on a long time to reach the temperature set-point. In Fig. 12, at maximum power about three seconds are taken to reach the temperature set-point. In this case, at the beginning of the test, an undesired area without hardening was produced.

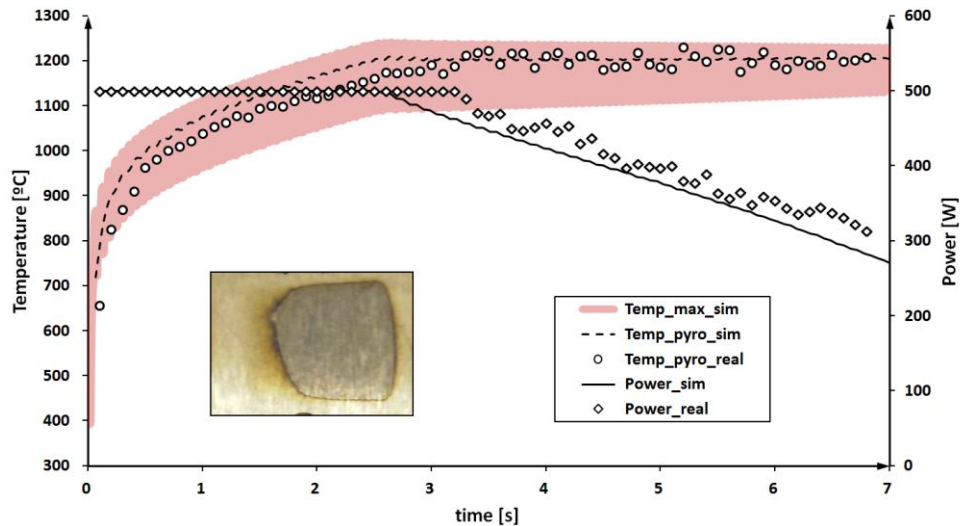


Fig. 12 Real/simulated temperature and power graphs during a test with  $K_p = 1.6$ ,  $K_d = 0.05$ ,  $K_i = 0$  and  $P_{sp} = 500$  W.

### 3. Temperature control results and discussion in real manufacturing parts

The temperature control developed and its parameters adjusting method was tested in complex geometry parts. Thus, LTHS process was used for test part hardening emulating stainless steel valves shafts and cast iron stamping dies, among other real manufacturing parts.

The LTHS tests have been performed in a 5 axis machine-tool with a workspace in X, Y, Z respectively of  $700 \times 400 \times 600$  mm<sup>3</sup> and two rotary axes, B and C. The spindle was replaced by a 2D scanner that can scan an area of  $120 \times 120$  mm<sup>2</sup>, which adds two additional linear axes, U and V. The laser system is a solid state fiber laser Rofin - Sinar FL010 with a maximum power of 1 KW, coupled to a 100 micron fiber coupled to the scanner. In the Fig. 13a) the laser processing machine used for the experiments is shown. The system combines 7 axes, the 5 axes of the machine (3 linear and 2 rotary), which can be considered as slow and long axes, and the two axes of the scanner, much faster and shorter. Thus, during the experimentation, the motion associated with the feed rate was made with the machine axes and the ones associated with the scanning speed with the 2D scanner axes.

#### LTHS process in stainless steel valves shafts

As an example of LTHS process application on real part cylindrical stainless steel valves shafts have been hardened. Valves were 13.3 mm in diameter and the material is a special stainless valve steel, X45CrSi9\_3. The axes configuration shown in Fig. 13b) was used for hardening tests. The feed rate was given by the B rotation axis of the laser machine and the scanning speed by the U axis of the scanner.



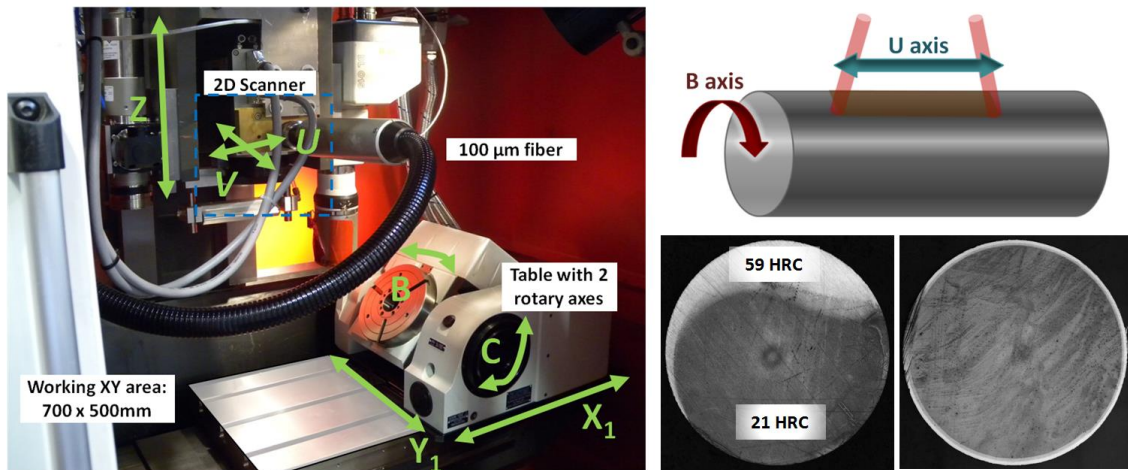


**Fig. 13** a) LTHS machine axes configuration; b) B axis and U axis during valves shafts hardening; c) Hardened layer obtained during LTHS process without temperature control; d) Hardened layer obtained during LTHS process with temperature control.

The analysis of the cross sections of different tests shows clearly the importance of temperature control. Thus, as it is shown in Fig. 13c), working without a temperature control involves a non-uniform hardened layer along the shaft periphery. In addition, two undesirable zones are observed, a non-hardened area at the beginning of the test and melted material at the last part of the test. On the other hand, the activation of the close loop temperature control allows a uniform hardened layer along the whole surface (Fig. 13d)).

Contrasting hardness values, the hardness obtained by LTHS process is near three times higher than the base material. A similar result is obtained with other conventional hardening processes.

#### LTHS process in cast iron stamping dies

As an example of LTHS process application with temperature control, a test-part emulating a stamping die has been hardened. The base material of the test-part is a nodular cast iron (DIN GGG70L EN-GJS-700-2L). The laser motion is obtained by a combination of X, Y and Z machine axes and U and V scanner axes. The hardened test-part is shown in Fig. 14. It represents a complex 3D part where the edges have been hardened.

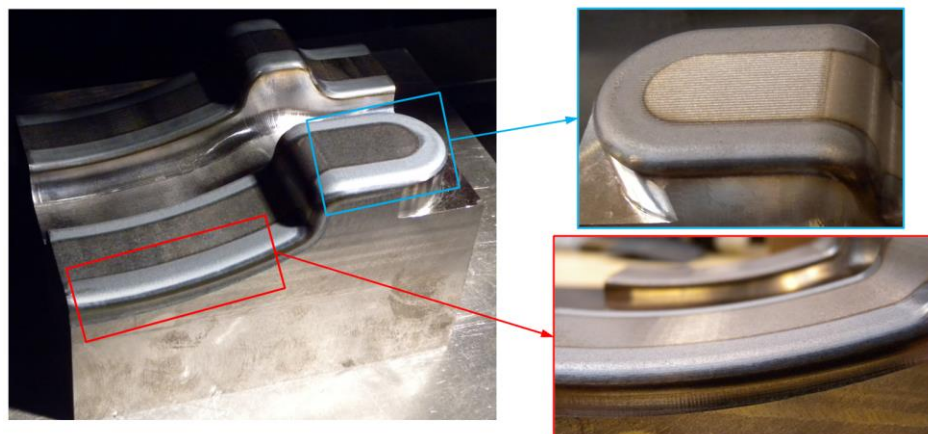


**Fig. 14** LTHS process with temperature control in a cast iron test-part emulating a stamping die.

The temperature control in nodular cast iron presents high instability due to noise at the temperature measurement. Graphite spheres at the cast iron surface present much higher absorption of the laser radiation than cast iron. Therefore, if the laser crosses a nodular graphite sphere in the point where the temperature is being measured, the actual temperature is rapidly increased and the pyrometer signal also presents a local peak. The result is that temperature signal present severe noise and an integral algorithm is needed for smooth the control of the temperature. In Fig. 15a) the temperatures in cast iron with PD tuned constants for steel are shown. By contrast, in Fig. 15b) the temperatures in cast iron with PID tuned constants for cast the iron are shown.

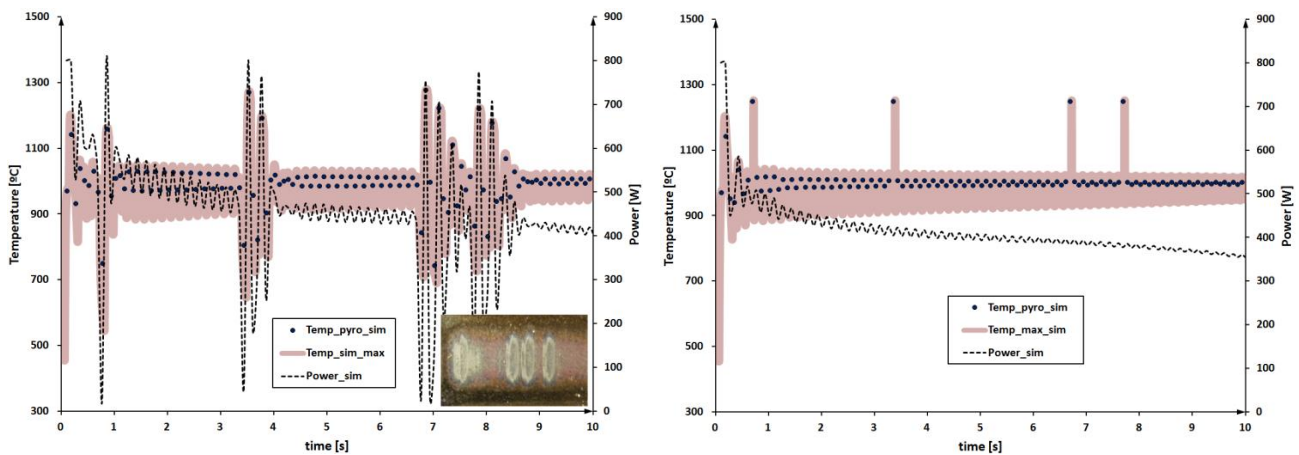


**Fig. 15 a)** Temperatures in cast iron with PD tuned constants for steel; **b)** Temperatures in cast iron with PID tuned constants for cast iron;

#### 4. Conclusions

Laser transformation hardening with scanning optics (LTHS) process is still an experimental process and presents a number of handicaps, especially regarding process temperature control, that reduce its industrial reliability. However, the scanning optics allows variable width areas, giving a high flexibility to the laser hardening process. Thus, there is a high interest on developing new solutions in order to establish LTHS as an industrial hardening process. The method proposed for temperature control for LTHS process and the results obtained are summarized below:

- A PID closed loop temperature control has been implemented in a laser machine for LTHS process. Due to the variability of the temperature field during the LTHS process a control loop of the temperature was considered.
- The temperature control has been tuned by means of numerical simulations of the system. The system consists of the simulated control and the simulated process.
- Validation tests have been carried on comparing real and simulated system with the same proportional, derivative and integrative constants for some specific experiments. The trend of the results in all cases is similar with slight variations between the simulated and real power. This is because the laser power is different to the power absorbed by the part because the power losses.
- LTHS process with the developed temperature control was used for hardening stainless steel valves shafts and cast iron stamping dies. The results present uniform hardened layers along the whole surface without unhardened or melted areas.



## Acknowledgments

The authors want to thank Ing. P. Hernandez for his support in this research work. Special thanks are addressed to the Industry and Competitiveness Spanish Ministry for the support on the DPI2013-46164-C2-1-R TURBO project.

## References

- [1] H. K. D. H. Bhadeshia. *Steels for bearings*. Progress in Materials Science, 57 (2012), 268-437. doi:10.1016/j.pmatsci.2011.06.002
- [2] T. Inoue. *Metallo-Thermo-Mechanical Coupling in Quenching*. Comprehensive Materials Processing, 12 (2014), 177-251. doi:10.1016/B978-0-08-096532-1.01206-1.
- [3] B. S. Yilbas, S. Akhtar, O. Keles. *Laser cutting of triangular blanks from thick aluminum foam plate: Thermal stress analysis and morphology*. Applied Thermal Engineering, 62 (2014), 28-36. doi:10.1016/j.applthermaleng.2013.09.026
- [4] M. Seifert, K. Anhalt, C. Baltruschat, S. Bonss, and B. Brenner. *Precise temperature calibration for laser heat treatment*. Journal of Sensors and Sensor Systems, 3 (2014), 47-54. doi:10.5194/jsss-3-47-2014
- [5] R. Poprawe. *Tailored Light 2 - Laser Application Technology*. Springer, (2011). doi:10.1007/978-3-642-01237-2
- [6] F. E. Pfefferkorn, N. A. Duffie, X. Li, M. Vadali, C. Ma. *Improving surface finish in pulsed laser micro polishing using thermocapillary flow*. CIRP Annals - Manufacturing Technology, 62 (2013), 203-206. doi:10.1016/j.cirp.2013.03.112
- [7] K. Kim, K. Yoon, J. Suh, J. Lee. *Laser Scanner Stage On-The-Fly Method for ultrafast and wide Area Fabrication*. Physics Procedia, 12 (2011), 452-458. doi:10.1016/j.phpro.2011.03.156
- [8] E. Díaz-Tena, A. Rodríguez-Ezquerro, L.N. López de Lacalle Marcaide, L. Gurtubay Bustinduy, A. Elías Sáenz. *A sustainable process for material removal on pure copper by use of extremophile bacteria*. Journal of Cleaner Production, 84 (2014), 752-760. doi:10.1016/j.jclepro.2014.01.061
- [9] J. Diaci, D. Bracun, A. Gorkic, J. Mozina. *Rapid and flexible laser marking and engraving of tilted and curved surfaces*. Optics and Lasers in Engineering, 49 (2011), 195-199. doi:10.1016/j.optlaseng.2010.09.003
- [10] H. Kangda, L. Geng, G. Ming, Z. Xiaoyan. *Weld formation mechanism of fiber laser oscillating welding of austenitic stainless steel*. Journal of Materials Processing Technology, 225 (2015), 77-83. doi:10.1016/j.jmatprotec.2015.05.021
- [11] I. Arrizubieta, A. Lamikiz, S. Martínez, E. Ukar, I. Tabernero, F. Girot. *Internal characterization and hole formation mechanism in the laser percussion drilling process*. International Journal of Machine Tools & Manufacture, 75 (2013), 55-62. doi: 10.1016/j.ijmachtools.2013.08.004
- [12] F. Klocke, C. Brecher, D. Heinen, C. J. Rosen, T. Breitbach. *Flexible scanner-based laser surface treatment*. Physics Procedia, 5 (2010), 467-475. doi:10.1016/j.phpro.2010.08.169
- [13] G. H. Farrahi, M. Sistaninia. *Thermal Analysis of Laser Hardening for Different Moving Patterns*. IJE Transactions A: Basics, 22 (2009), 169-180.
- [14] H. W. Song, S. X. Li, L. Zhang, G. Yu, L. Zhou, J. S. Tan. *Numerical simulation of thermal loading produced by shaped high power laser onto engine parts*. Applied Thermal Engineering, 30 (2010), 553-560. doi:10.1016/j.applthermaleng.2009.10.018
- [15] T. Purtonen, A. Kalliosaari, A. Salminen. *Monitoring and adaptive control of laser processes*. Physics Procedia, 56 (2014), 1218-1231. doi:10.1016/j.phpro.2014.08.038
- [16] F. Valiorgue, A. Brosse, P. Naisson, J. Rech, H. Hamdi, J. M. Bergheau. *Emissivity calibration for temperatures measurement using thermography in the context of machining*. Applied Thermal Engineering, 58 (2013), 321-326. doi:10.1016/j.applthermaleng.2013.03.051
- [17] J. R. Lawrence, J. Pou, D. K. Y. Low, E. Toyserkani. *Advances in Laser Materials Processing: Technology, Research and Application*, Woodhead Publishing. ISBN 978-1-84569-474-6, (2010). doi:10.1533/9781845699819.4.291
- [18] D. Hömberg, W. Weiss. *PID Control of Laser Surface Hardening of Steel*. IEEE transactions on control systems technology, Vol. 14 - Nº5, (2006), 896-904. doi: 10.1109/TCST.2006.879978

- [19] B. Sinkovics, P. Gordon, G. Harsányi. *Computer modelling of the laser ablation of polymers*. Applied Thermal Engineering, 30 (2010), 2492-2498. doi:10.1016/j.applthermaleng.2010.06.022
- [20] T. Amine, J. W. Newkirk, F. Liou. *Investigation of effect of process parameters on multilayer builds by direct metal deposition*. Applied Thermal Engineering, 74 (2014), 500-511. doi:10.1016/j.applthermaleng.2014.08.005
- [21] Y. C. Yuan, C. W. Wu. *Thermal analysis of film photovoltaic cell subjected to dual laser beam irradiation*. Applied Thermal Engineering, 88 (2015), 410-417. doi:10.1016/j.applthermaleng.2015.01.054
- [22] J.G. Ziegler, N.B. Nichols, N.Y. Rochester. *Optimum Settings for Automatic Controllers*. Transactions of the A.S.M.E., November (1942), 759-768.
- [23] W. Devesse, D. De Baere, P. Guillaume. *Design of a model-based controller with temperature feedback for laser cladding*. Physics Procedia, 56 (2014), 211-219. doi:10.1016/j.phpro.2014.08.165
- [24] P. Zhang. *Advanced Industrial Control Technology*. Elsevier. Chapter 19, (2010). doi:10.1016/B978-1-4377-7807-6.10019-1
- [25] R. F. Brito, S. R. Carvalho, S. M. M. Lima, E. Silva. *Experimental investigation of thermal aspects in a cutting tool using comsol and inverse problem*. Applied Thermal Engineering, 86 (2015), 60-68. doi:10.1016/j.applthermaleng.2015.03.083
- [26] K. J. Astrom, T. Hagglund. *Advanced PID Control*. ISA-The Instrumentation, Systems and Automation Society, (2006).
- [27] J. Thevenet, M. Siroux, B. Desmet. *Measurements of brake disc surface temperature and emissivity by two-color pyrometry*. Applied Thermal Engineering, 30 (2010), 753-759. doi:10.1016/j.applthermaleng.2009.12.005
- [28] E. Ukar, A. Lamikiz, L.N. López de Lacalle, S. Martinez, F. Liébana, I. Tabernero. *Thermal model with phase change for process parameter determination in laser surface processing*. Phys Procedia, 5 (2010), 395-403. doi:10.1016/j.phpro.2010.08.066